
ASTRO-H

# INSTRUMENT CALIBRATION REPORT
# SXS GATE VALVE WINDOW TRANSMISSION
# ASTH-SXS-CALDB-GATEVALVE

Version 0.3

07 November 2016

**ISAS/ GSFC**

**Prepared by:** Megan Eckart, Maurice Leutenegger, Caroline Kilbourne, Maxim Markevitch (GSFC); A. Hoshino, S. Kitamoto (Rikkyo University); R. Fujimoto (Kanazawa University); and the SXS Instrument Team

# Table of Contents

# CHANGE RECORD PAGE (1 of 1)

| DOCUMENT TITLE: SXS Gate Valve Window Transmission | | | |
|---|---|---|---|
| ISSUE | DATE | PAGES AFFECTED | DESCRIPTION |
| Version 0.1 | March 2016 | All | First Release |
| Version 0.2 | August 2016 | All | Initial update based on in-flight data CALDB release 20160606 |
| Version 0.3 | November 2016 | All | Update based on measurements of spare Be window. CALDB release 20161027 |

# Introduction

## 1.1 Purpose

During the Astro-H commissioning observations the SXS dewar gate valve (GV) remained closed to protect the instrument from initial spacecraft outgassing. As a result, the optical path of the observations included the beryllium window installed on the GV. This ~260 micron-thick window absorbs a large fraction of the x-ray photons at energies below 2 keV. In addition, associated metal support structures attenuate approximately half of the x-ray flux across the science bandpass.

This document describes the transmission of the beryllium window and associated protective metal mesh. We describe the window geometry, materials, and calculation of the resulting x-ray transmission as a function of energy. The GV also includes a cross structure that attenuates a significant fraction of incident photons. To calculate the obscuration by the cross requires ray tracing; it is therefore not discussed in this document and instead is described in ASTH-SXS-CALDB-RAYTRACE by T. Yaqoob et al.

## 1.2 Scientific Impact

For observations that took place during the gate-valve-closed phase the gate valve CALDB file is used in the Ancillary Response Function (ARF) calculation for spectral analysis and in the flat field for imaging analysis.

# 2 Release CALDB 20161122

| Filename | Valid data | Release data | CALDB Vrs | Comments |
|---|---|---|---|---|
| ah_sxs_gatevalv_20140101v003.fits | 2014-01-01 | 20161122 | 005 | Extension 2 (Extensions 1 & 3 are described elsewhere.)<br><br>Original ASCII file for Extension 2: trans_GVBeWithMesh_SXS_SpareBe_v0.txt |

The gate valve remained closed for the entirety of the Astro-H mission lifetime, and thus the gate valve window was in the optical path for all SXS observations. In this release of the CALDB we incorporate synchrotron measurements of the flight-spare Be window, which was from the same lot of material as the flight Be window. Ref. [8] presents details of the measurements and associated modeling. Here we summarize the measurements and results that were used in generating the CALDB file.

## 2.1 Data Description

Both x-ray fluorescence (XRF) analysis and x-ray transmission measurements were performed in June 2016 on the flight-spare Be window at SPring-8, a synchrotron operated by the Japan Synchrotron Radiation Research Institute (JASRI).

The XRF measurements were performed with a 19-SSD Ge detector and showed the presence of Mn, Cr, Fe, Ni, and Cu contaminants. The Fe and Ni K-lines were strong, the Mn K-line was weak, and the Cr and Cu K-lines were very weak. The JAXA memo [8] shows examples of the XRF measurements.

The x-ray transmission measurements were performed at beamline BL01B1 by T. Uruga and T. Ina, from 10:00 June 15, 2016 to 10:00 June 17, 2016 JST. The beamline operating range is 3.8–30 keV. We used a beam spot size of 1 mm x 0.2 mm to measure two positions on the Be window, at the center of the window and at one position 6.5 mm off-center. Each of these data sets was accompanied by a measurement where the window was removed from the beam path. These measurements were taken in 21 separate energy ranges covering 3.8–30 keV total, each with overlap of 0.5 keV. Five sets of measurements were taken at each energy range, so 105 files total (21 energy ranges x 5 datasets) with 3 measurements (2 positions on the window + 1 calibration measurement) per file. We used simultaneous transmission measurements of standard materials for energy calibration.

## 2.2 Data Analysis

The transmission data clearly showed Fe and Ni K-edges, plus a marginal detection of the Mn K-edge. In addition, there were edge-like features observed at 6057 eV and 6915 eV, plus very weak edge-like features at 7590 eV and 9193 eV, which are labeled 'unknown edges' in Ref. [8] since they do not correspond to edge-energies of any atomic absorption edges.

Using the online Bragg planes tool [9] we determined that the energies of these unknown edges are consistent with the energies that correspond to the minimum allowed energy for Bragg diffraction from the (1,-1,0,3), (0,0,0,4), (1,0,-1,4), and (1,0,-1,5) planes of Be. The Bragg plane tool gives corresponding energies of 6060 eV, 6918 eV, 7588 eV, and 9191 eV. Above each energy Bragg diffraction is allowed for the corresponding plane. We posit that because the material is polycrystalline all Bragg angles and thus all diffracted energies are sampled, so that the effect looks like an edge in transmission. We caution that we have not performed calculations to verify if the relative edge strengths are reasonable and whether it makes sense to observe these edges and not others. Edges at the 2d for the (2,-1,1,1) / 5690 eV; (2,-1,1,0) / 5420 eV; and (1,0,-1,2) / 4665 eV planes would be expected, but were not observed. The edge strengths may be too low for these features. Other potential edges in the science band of the SXS fall below the 3.8 keV minimum energy of the synchrotron measurements, including scattering from the (1,0,-1,1) / 3575 eV; (0,0,0,2) / 3460 eV; and (1,0,-1,0) / 3129 eV planes.

We found that our transmission data was best fit using the following components:

- photoabsorption by Be plus contaminants (Ni, Fe, Cu, Mn, Cr) using literature values of the mass absorption coefficients provided in Ref. [1]
- incoherent scattering by Be, using $\mu_{inc}$ provided on page 305 of Ref. [1]
    - note: Ref [1] reports $\mu_{inc}$ of 0.142–0.173 $cm^2/g$ for the energy range of 7–30 keV
- edges at 6057 eV and 6915 eV, which we ascribe to Bragg diffraction by the (polycrystalline) Be

We calculate the transmission of each material due to photoabsorption as usual:

$$T(E) = \exp(-\mu(E) * t) \ , \qquad \textbf{Eq. ( 1 )}$$

where $\mu(E)$ is the mass attenuation coefficient as a function of x-ray energy and $t$ is the thickness.

For Be, the photoabsorption cross section dominates the total absorption cross section to ~7 keV, above which the contribution of incoherent scattering becomes significant. We calculate the contribution due to incoherent scattering using

$$T(E) = \exp(-\rho * \mu_{inc} * t) \ , \qquad \textbf{Eq. ( 2 )}$$

where $\mu_{inc}$ is the cross section of incoherent scattering, $\rho$ is the density, and $t$ is the thickness.

Finally, we model the unknown edges with $T(E)=1$ for $E<E_c$ and

$$T(E) = \exp\left(-D\left(\frac{E}{E_c}\right)^{-3}\right) \qquad \textbf{Eq. ( 3 )}$$

for $E>E_c$, where $D$ is the edge depth and $E_c$ is the edge energy. We found that all of these components are needed to fit the data. For example, without the incoherent scattering then an overall scale factor must be applied to fit the data. And without the unknown edges, the best-fit model over predicts the K-edge depths of Mn, Fe, and Ni.

The best-fit model parameters are presented in Table 1.

| Element | Density [g/cm$^3$] | Best-fit Thickness | Best-fit Edge Depth | Comment |
|---|---|---|---|---|
| Be | 1.85 | 261.86 ± 0.01 μm | | Plus include incoherent scattering, with $\mu_{inc}$ from p305 of Ref. [1] |
| Cr | 7.190 | 3 nm (fixed) | | |
| Mn | 7.30 | 3.81 ± 0.05 nm | | |
| Fe | 7.874 | 10.83 ± 0.05 nm | | |
| Ni | 8.902 | 16.48 ± 0.03 nm | | |
| Cu | 8.960 | 5 nm (fixed) | | |
| 6.057 keV | | | 2.194 ± 0.02 x $10^{-3}$ | attributed to Bragg scattering from (polycrystalline) Be |
| 6.915 keV | | | 0.867 ± 0.03 x $10^{-3}$ | attributed to Bragg scattering from (polycrystalline) Be |

**Table 1** Best-fit Be window model parameters based on measurements of spare window.

## 2.3 Results

For Extension 2 we provide two columns: x-ray energy and transmission. The energy range is 10 to 40000 eV with a step size of 0.25 eV. We use the best-fit model parameters of Table 1 to create the Be window transmission curve from 10–30000 eV, and set the transmission from 30–40 keV equal to the (near-unity) transmission at 30 keV. We combine this Be window transmission curve with the effects of the stainless steel mesh (see details in Section 4.2) to produce the final transmission curve for the CALDB.

The blue curve in Figure 4 shows the results from 1–12 keV, while Figure 2 shows the transmission curve over the extended energy range.

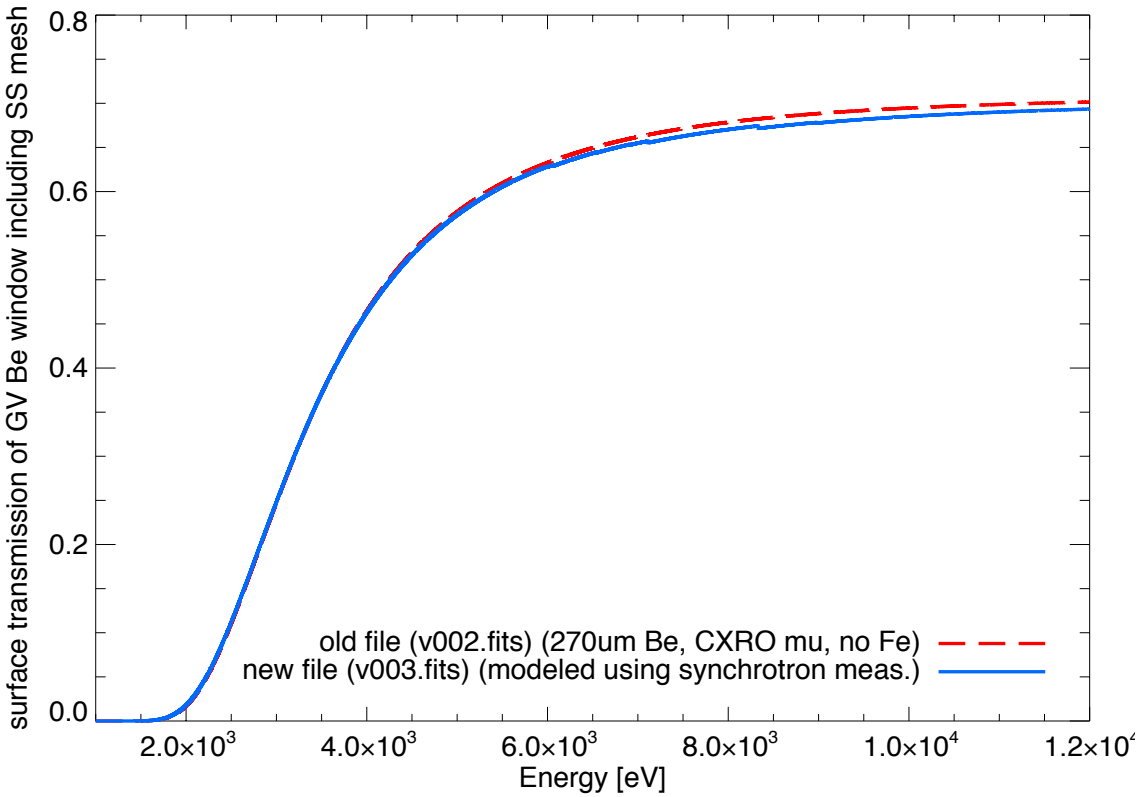


**Figure 1** The blue curve shows the transmission from 1–12 keV based on the synchrotron measurements of the spare Be window after incorporating the effects of the protective stainless steel mesh. These data are incorporated in CALDB release 20161027. The red dashed curve presents uses the previous version of the CALDB (20160606), which was based on initial fits to the in-orbit astronomical data as described in Section 3.

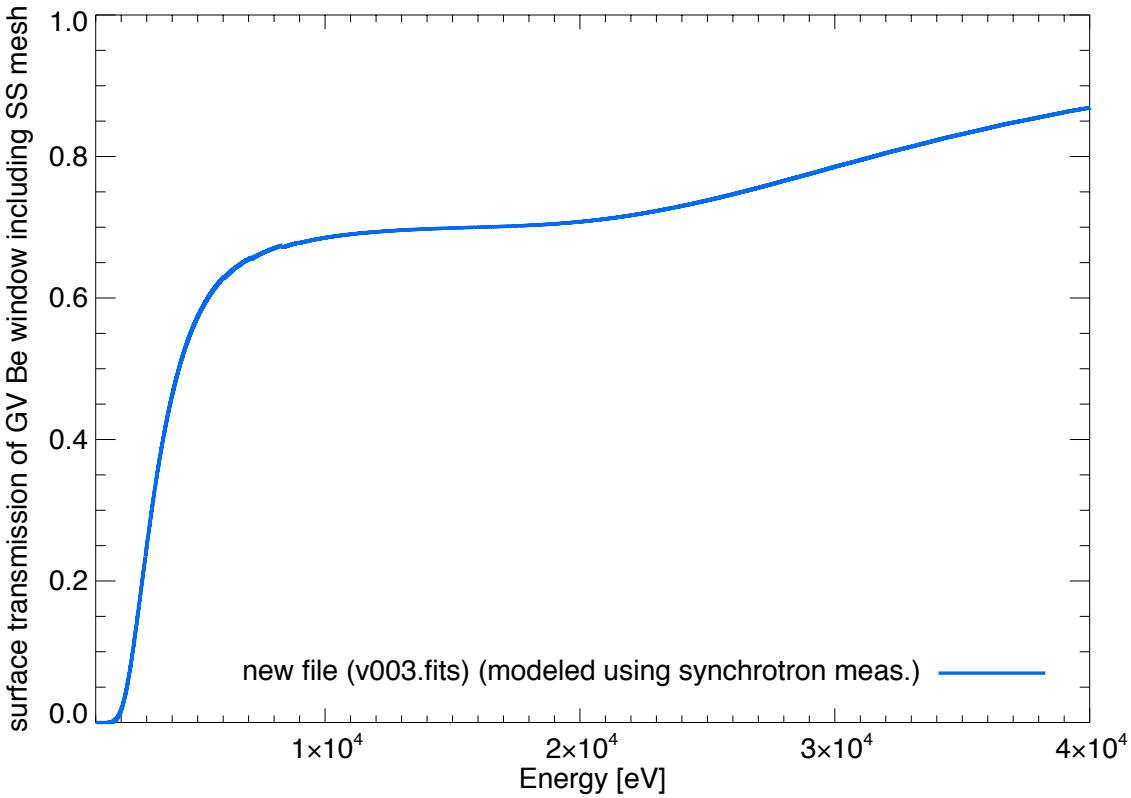


**Figure 2** Transmission over the extended energy range, to 40 keV.

## 2.4 Comparison with previous release

Figure 1 provides a comparison of the updated transmission to the previous release; Table 2 highlights the differences at selected energies.

| **Energy** | **Surface Transmission** | |
|---|---|---|
| [eV] | Previous Release (v002.fits) | Updated File (v003.fits) |
| 2000 | 0.0172 | 0.0180 |
| 3000 | 0.247 | 0.248 |
| 4000 | 0.464 | 0.463 |
| 5000 | 0.577 | 0.574 |
| 8000 | 0.679 | 0.670 |
| 10000 | 0.695 | 0.685 |
| 12000 | 0.702 | 0.693 |

**Table 2** Extension 2 of the CALDB file at selected energies, comparing the previously released file (20160606) to the updated file (20161027).

# 3 Release CALDB 20160606

| Filename | Valid data | Release data | CALDB Vrs | Comments |
|---|---|---|---|---|
| ah_sxs_gatevalv_20140101v002.fits | 2014-01-01 | 20160606 | 003 | Extension 2 (Extensions 1 & 3 are described elsewhere.)<br><br>Original ASCII file for Extension 2: trans_GVBeWithMesh_SXS_v3.0.txt |

The gate valve remained closed for the entirety of the Astro-H mission lifetime, and thus the gate valve was in the optical path for all SXS observations. In order to extract the maximum science output from the limited number of observations performed, we provide an updated transmission file based on estimates from in-orbit data.

## 3.1 Data Description

The x-ray transmission of the Be window was not calibrated prior to launch owing to a combination of schedule constraints and our intention to remove the window from the optical path prior to the on-orbit calibration and science observation phases. Prior to launch (for CALDB 20160310 release), we calculated the transmission of the window based upon the nominal Be window thickness of 300 microns and nominal geometry and material properties of the metal support mesh. The details of this pre-launch approach, including detailed descriptions of the metal support structures, is documented in Section 4.

Following launch, we received additional information that suggested a revised estimate of the Be window thickness was required. First, we were recently provided with a manufacturer-supplied data sheet from November 2010, which indicated that the Be window thickness was in the range of 274–290 μm, significantly thinner than the nominal 300 μm used for the pre-flight CALDB file. The data sheet also indicated Ni and Fe impurities at levels of $\leq 0.02\%$ and $\leq 0.03\%$ respectively. We do not have access to these data (methods, uncertainties, etc.), so cannot quantify the expected thickness nor the uniformity of the Be or the uncertainties on the material composition. Second, we acquired SXS data of two astronomical continuum sources, G21.5-09 and the Crab pulsar. Combining these data with models of the source spectral shape from the literature allows an estimate of the thickness of the Be window.

## 3.2 Data Analysis

We jointly modeled the observed spectra of the Crab and G21.5-0.9, using a model with Be thickness as a free parameter. The model also included an overall scale factor for the flux of each source spectrum.

We analyzed the Crab data with Hitomi software release V001. We screened the data using the anti-coincidence detector but did not perform pixel-to-pixel coincidence screening nor account for lost event GTI. Since we include an overall scale factor on the flux during the final modeling, our ignoring the lost event GTI will not affect the final results, despite the presence of lost events in this bright-source dataset. For the G21.5-09 data we analyzed the data using the NASA/GSFC

SXS instrument team software suite, XRSGSE Version 10.7.6b1. Again, we screened events using the anti-coincidence detector.

The model-derived Be thickness is mildly influenced by the method of modeling of the energy-loss continuum. See Ref. [6] for an example of the energy-loss processes, due to either electron or photon escape, that can occur during the rapid thermalization process that takes place in the HgTe absorber following x-ray absorption. We do not currently have adequate models of the pre-flight measurements of these loss processes, so we characterized the energy-loss continuum empirically with a power law model. The results of the fitting are shown in Figure 3. **The derived Be thickness is 270 µm ± 10 µm (statistical).** We estimate that a 10 µm systematic error may be introduced by our method of modeling the electron loss continuum. These results and Figure 3 are also presented in Ref. [7].

Since the manufacturer-supplied material composition data indicate that there could be Ni or Fe at the ~0.02% level, we also checked to see whether the observational data was better fit with models that included thin layers of those elements. We found that the absence of a 7.1 keV edge in the Crab data constrains the Fe composition to be <0.01% at 90% confidence. A composition of 0.01% Fe only affects the transmission at <2.5 keV by ~2%, so we assume the window has negligible Fe impurities. The Ni is harder to constrain from the available data, and so for this initial update to the pre-flight transmission we again decided to assume the level of Ni impurities is negligible. This assumption will be revisited in the future if necessary.

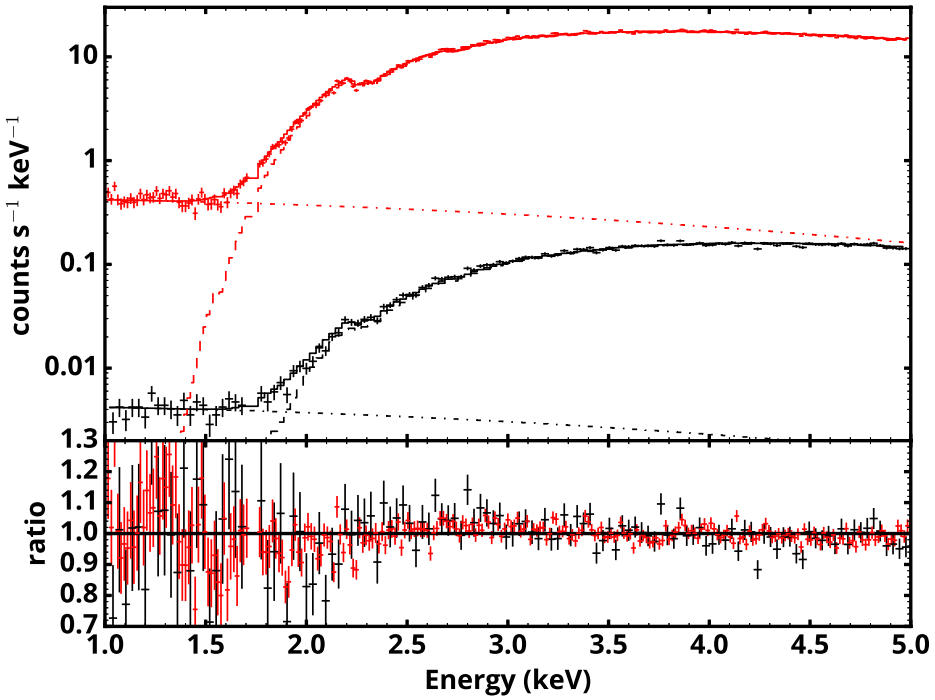


**Figure 3** (Figure 7 of Ref. [7]) Joint model (solid lines) fit to SXS observations (point with error bars) of the Crab pulsar (red) and G21.5-0.9 (black). The best fit model (dashed line) for each source was allowed to vary while varying a single parameter for the Be window thickness in both observations. The energy loss continuum (dash-dot line) is empirically fit in each source as a separate power law. The ratio of data to model is shown in the bottom panel.

### 3.3 Results

For Extension 2 we provide two columns: x-ray energy and transmission. The energy range is 10 to 40000 eV with a step size of 0.25 eV. We calculate this transmission of the gate valve Be window, including the effects of the stainless steel support mesh, using the best-fit Be thickness based on the in-flight data. The procedure is the same as described in Section 4.2, with the following differences:

- we use the CXRO-derived mass attenuation coefficients to calculate the Be transmission across the entire bandpass (assuming no significant Fe impurities);
- we use a Be thickness of 270 μm instead of 300 μm.

The red curve in Figure 4 presents the results from 1–12 keV.

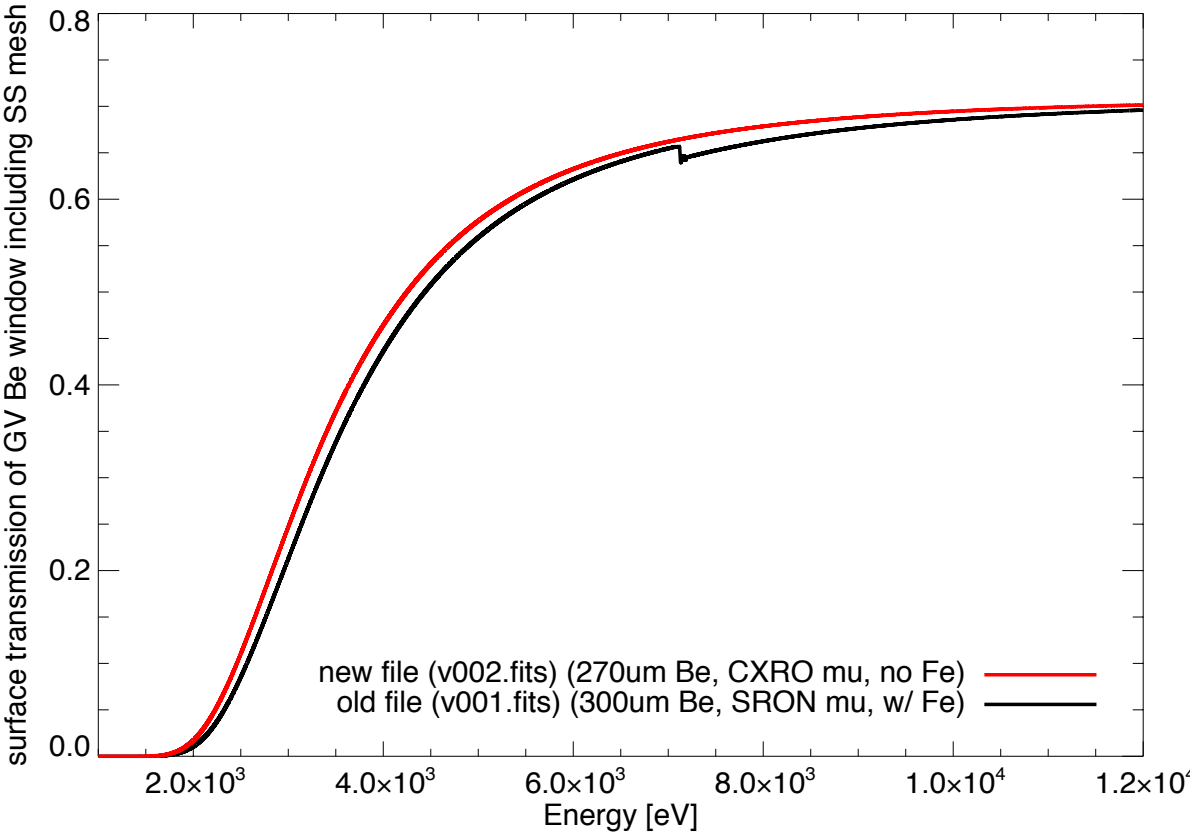


**Figure 4** The red curve shows the transmission from 1–12 keV based on the initial in-flight measurements. The black curve shows pre-flight best-estimate of the transmission as described in Section 4.

### 3.4 Comparison with previous release

Figure 4 provides a comparison of the updated transmission compared to the previous release; Table 3 highlights the differences at selected energies.

| Energy | Surface Transmission | |
|---|---|---|
| [eV] | Previous Release (v001.fits) | Updated File (v002.fits) |
| 2000 | 0.0104 | 0.0172 |
| 3000 | 0.213 | 0.247 |
| 4000 | 0.436 | 0.464 |
| 5000 | 0.559 | 0.577 |

**Table 3** Extension 2 of the CALDB file at selected energies, comparing the previously released file (20160310) to the updated file (20160606).

# 4 Release CALDB 20160310

| Filename | Valid data | Release data | CALDB Vrs | Comments |
|---|---|---|---|---|
| ah_sxs_gatevalv_20140101v001.fits | 2014-01-01 | 20160310 | 001 | Extension 2 (Extensions 1 & 3 are described elsewhere.)<br><br>Original ASCII file for Extension 2: trans_GVBeWithMesh_SXS_v2.0.txt |

### 4.1 Data Description

Table 4 summarizes the materials and dimensions of the GV window provided by JAXA and Sumitomo Heavy Industries, and Table 5 provides the position of the GV components with respect to the SXS detector plane. Figures 1–4 present drawings of the GV structures.

| Description | Material | Geometry | Thickness | Comments |
|---|---|---|---|---|
| | | | | |
| Be window | Be | uniform | 300 μm | No x-ray calibration measurements performed. |
| Protective mesh | stainless steel: SUS304 | 1/20-inch pitch wire mesh | Wire thickness = 0.20 mm | Mesh opening width is 1.27 mm – 0.20 mm = 1.07 mm<br>Open fraction = 71% |
| Support cross | aluminum alloy: A6061-T6 | cross with 2 mm-wide bars | 6 mm thick | Opaque in SXS science waveband. Aligned with SXT quadrant gaps, but blocks approx. 23%. |

**Table 4** Summary of gate valve Be window materials and dimensions. These information are documented in the SXS dewar description document, JAXA-XCS-C-001. The Be window is manufactured by Brush Wellman Ltd., which is now a part of Materion Corp.

| Feature | Height Above Detector Plane | Offset in S/C X, Y from Detector Center | Comments |
|---|---|---|---|
| | | | |
| Be window | ~243.85 mm | n/a | |
| Protective mesh | 247.9 mm | n/a | |
| Support cross | 243.9 mm (bottom of cross)<br>249.9 mm (top of cross) | -0.051mm, +0.221 mm (same as alignment pole) | These dimensions are input for raytracing code (to generate Ext. 1 & 3 of CALDB file). |
| GV aperture | 216 mm | n/a | |
| Top of GV alignment pole | 255.9 mm | -0.051mm, +0.221 mm | |

**Table 5** Positions of relevant GV components with respect to the SXS detector array. The heights are derived from mechanical drawings (see subsequent figures). The offset in X, Y are derived from alignment measurements summarized in document 150227_alignment_toNEC.pdf, provide by Yoh Takei (private communication, May 2015).

.

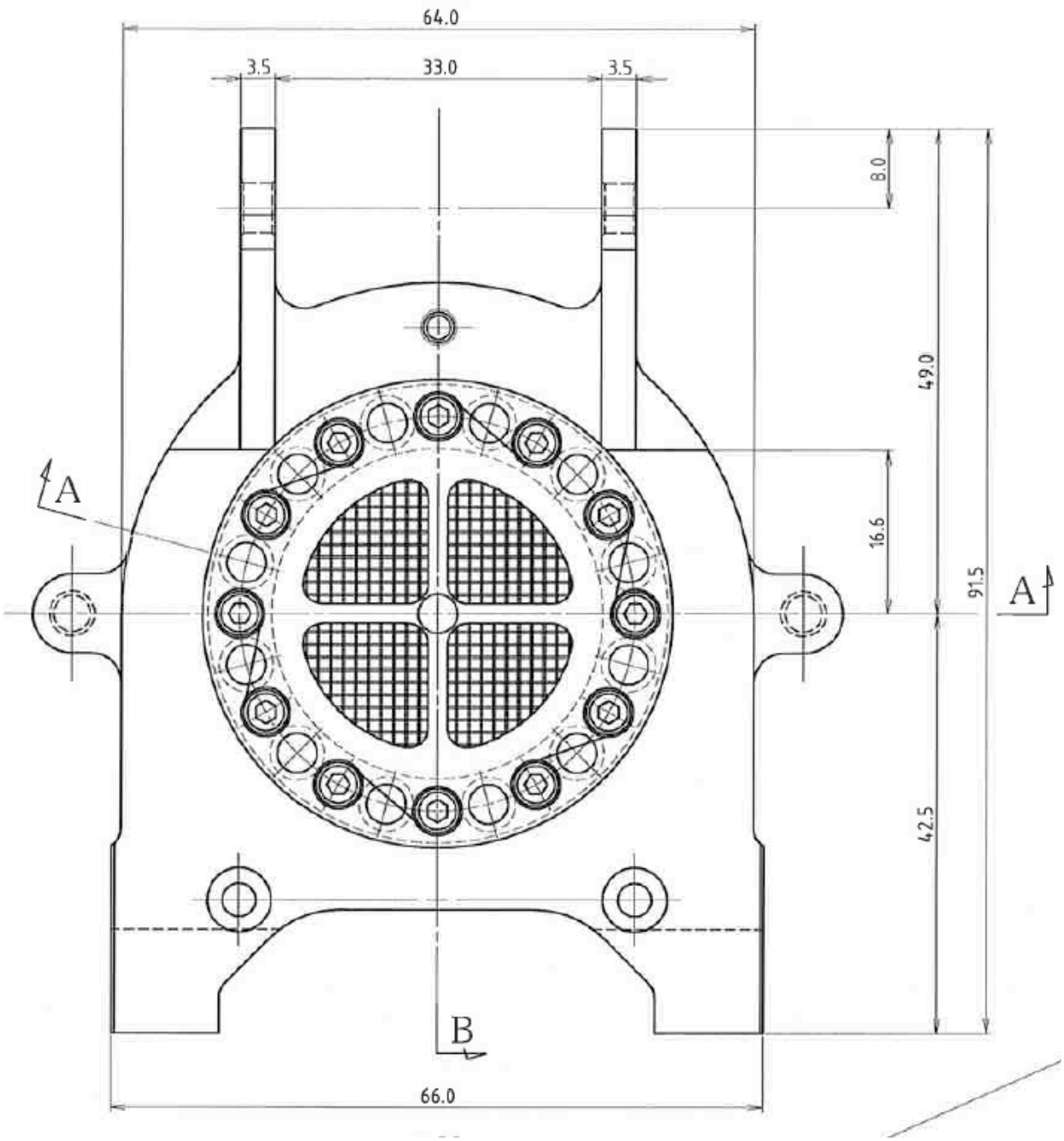


**Figure 5** Drawing of gate valve window support structure, including stainless-steel cross and mesh. This figure is a portion of SHI drawing KK0391T.

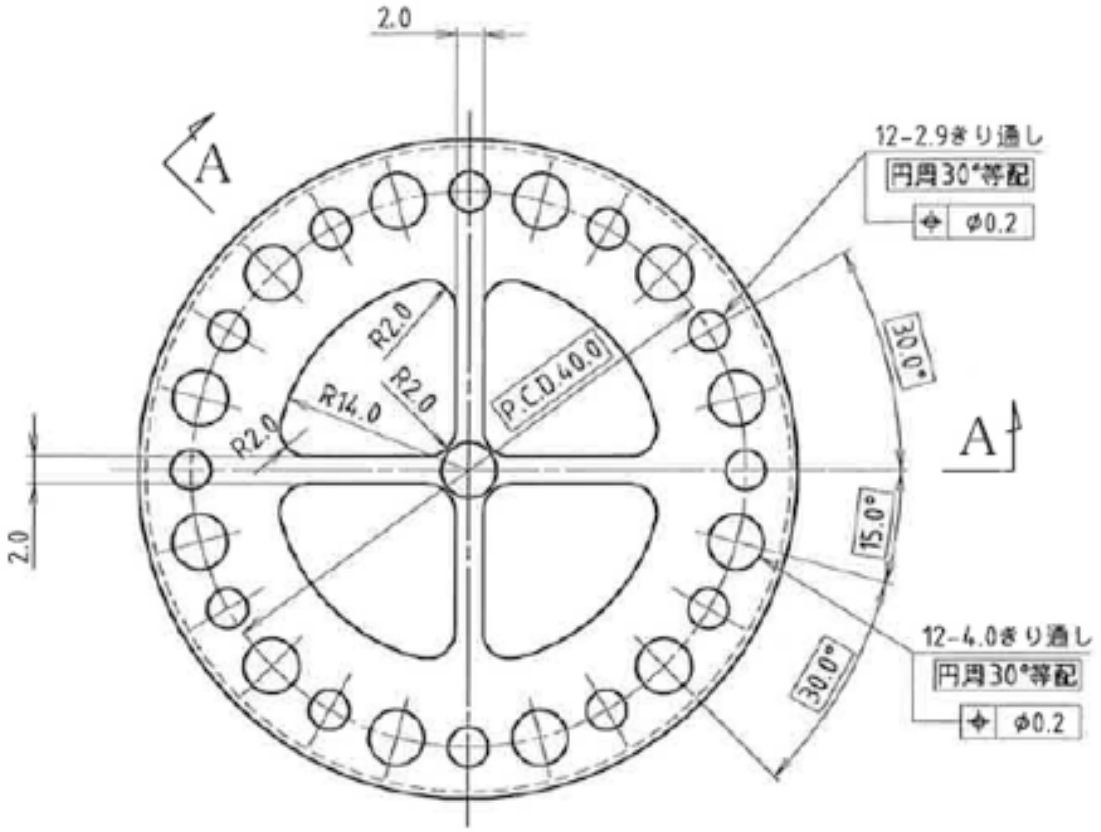


**Figure 6** Drawing of gate valve window support cross with dimensions.

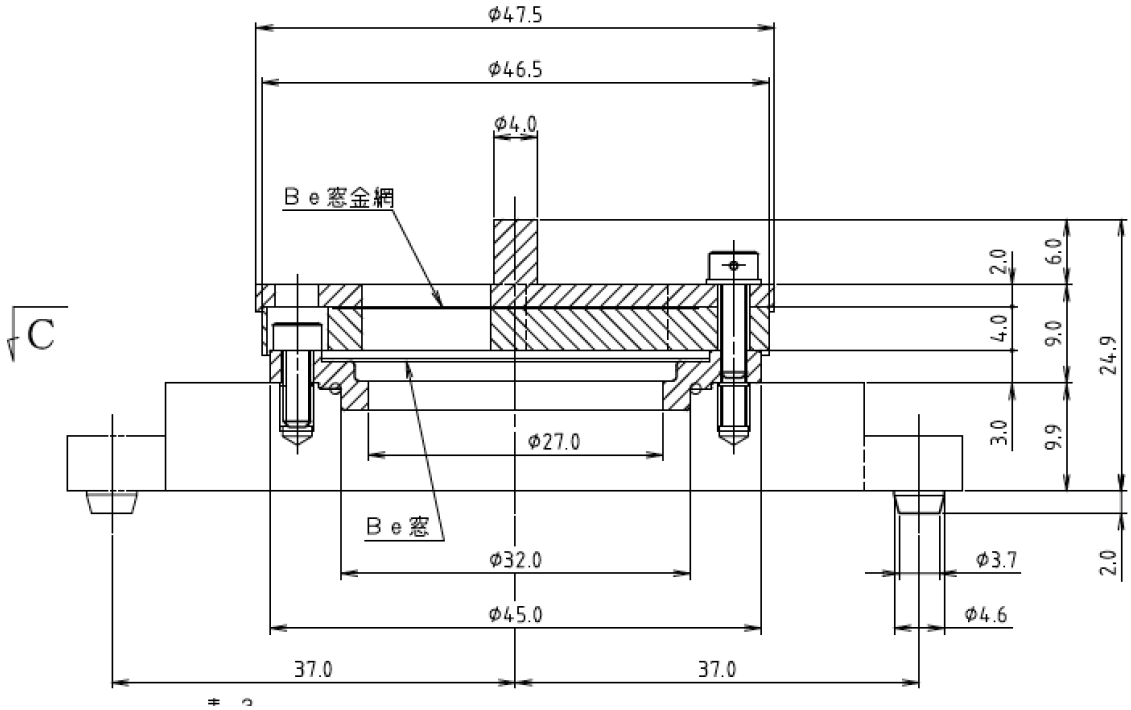


**Figure 7** Cross section of gate valve window support structure. This figure is a portion of SHI drawing KK0391T. The Be sits beneath the 6 mm-thick (4 mm + 2 mm) cross structure.

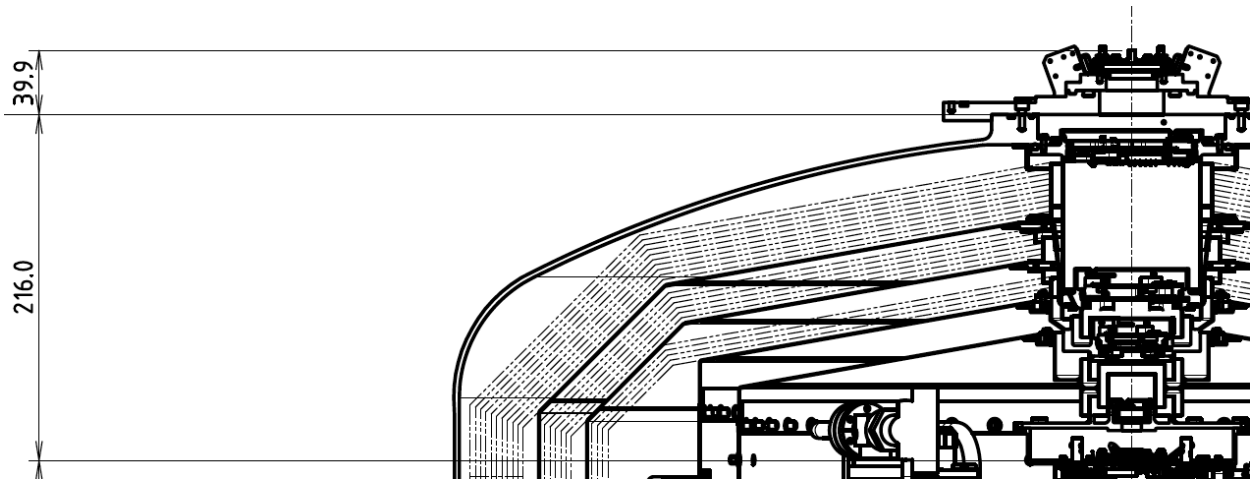


**Figure 8** Cross section of top portion of SXS dewar, showing that the GV aperture is 216 mm above the detector plane and the top of the GV pole is 39.9 mm above the GV aperture. These dimensions may be used to relate the drawing presented in **Figure 7** to the detector plane.

## 4.2 Data Analysis

The transmission given in Extension 2 of the CALDB file is labeled a 'surface transmission,' referring to the transmission through the components distributed across the surface of the GV aperture, namely the Be itself and the protective mesh. Given the size of the converging x-ray beam, the mesh geometry, and the size of the SXS detector pixels an average transmission is sufficient and a two-dimensional transmission map is not required. Thus the resulting 'surface transmission' is a product of the transmissions of the Be and the stainless steel mesh. In the following pages we describe how we calculate the transmission of each material and how they are combined to produce the final transmission.

**Transmission of the Beryllium Window:**

No x-ray calibration measurements were performed on the gate valve beryllium window owing to instrument schedule constraints. We therefore base our transmission estimates on the nominal manufacturer specifications combined with the complementary calibration measurements of the SXS filter wheel (FW) Be filter, which was supplied by the same manufacturer (Brush Wellman / Materion Corp.). Members of the SXS team calibrated FW Be filters (~27μm thickness) at BESSY. The inferred mass attenuation coefficients were consistent with literature values for Be (Ref. [1]) plus small edges due to Fe impurities. Ref. [2] summarizes the FW filter calibration campaign.

We assume that the GV Be window has a similar level of Fe impurities as the FW Be window, and thus need to include the Fe K-edge at ~7.1 keV. To do so we take the following approach: for energies below 14.8 keV we use the mass attenuation coefficients provided by SRON in Be-SN2-1-036.FIT (Ref. [2]), which include the Fe K-edge, while for energies from 14.8–40 keV we use the data from CXRO and our power-law extrapolation as described in the subsequent paragraph.

The Center for X-ray Optics (CXRO) at Lawrence Berkeley National Laboratory provides atomic scattering factor data for Be from 0.01–30 keV (see Ref. [1]). We used these data to calculate the Be photoabsorption cross sections and mass attenuation coefficients from 0.01–30 keV, and interpolated these data to provide a step size of 0.25 eV. The interpolation was linear in $\mu*E\hat{}2.5$, which was found to be well behaved. We fit the L-shell cross-section data from 25–30 keV with a power-law index of -3.33, and used this function to extrapolate the data to 40 keV.

The SRON FW Be measurements run from 400.57 eV to 14809.0 eV in 282 logarithmically spaced steps, but with 2 eV spacing from 7080–7200 eV to describe the Fe K-edge. We use a linear interpolation to bin these data on a 0.25 eV grid. At 400 eV the transmission of 300μm of Be is 10^-19, and thus we set the window transmission to 0 for energies below 400 eV.

We calculate the transmission using the following equation,

$$T(E) = \exp(-\mu(E) * t) \ , \qquad \textbf{Eq. ( 4 )}$$

where $\mu(E)$ is the mass attenuation coefficient as a function of x-ray energy and $t$ is the nominal Be thickness of 300 μm.

**Transmission of the Stainless Steel Mesh:**

The chemical composition of SUS304 is ~70% Fe, 18–20% Cr, and ~10 Ni and small fractions of other materials (a combination of Mn, N, Si, C, P, S). For this calculation we assume the mesh is 70% Fe, 20% Cr, and 10% Ni and composed of wires that have a square cross section of 0.2 mm x 0.2 mm.

We obtain the mass attenuation coefficient for Fe, Cr, and Ni from 2–45 keV using the X-ray Form Factor, Attenuation, and Scattering Tables available via the NIST Physical Measurement Laboratory (see References [3]-[5]) and linearly interpolate these data to provide mass attenuation coefficients on a 0.25 eV grid.

We calculate the transmission of the stainless steel bars of the mesh using Eq. (4) and a thickness of 0.2 mm. Note that over the primary SXS science bandpass (0.3–12 keV) the mesh wires are opaque.

**Combining transmissions to calculate the total 'surface transmission':**

The total 'surface transmission' is given by:

$$T_{total}(E) = T_{Be}(E) * (1 - f_{mesh}) + T_{Be}(E) * T_{mesh}(E) * f_{mesh} \qquad \textbf{Eq. ( 5 )}$$

,

where $T_{Be}$ is the Be transmission, $T_{mesh}$ is the stainless steel bar transmission, and $f_{mesh}$ is the geometric covering fraction of the mesh.

### 4.3 Results

In Extension 2 we provide two columns: x-ray energy and transmission. The energy range is 10 to 40000 eV with a step size of 0.25 eV. Figure 9 illustrates the results and Figure 10 shows the data on a log-log scale over the science waveband.

### 4.4 Final Remarks

None.

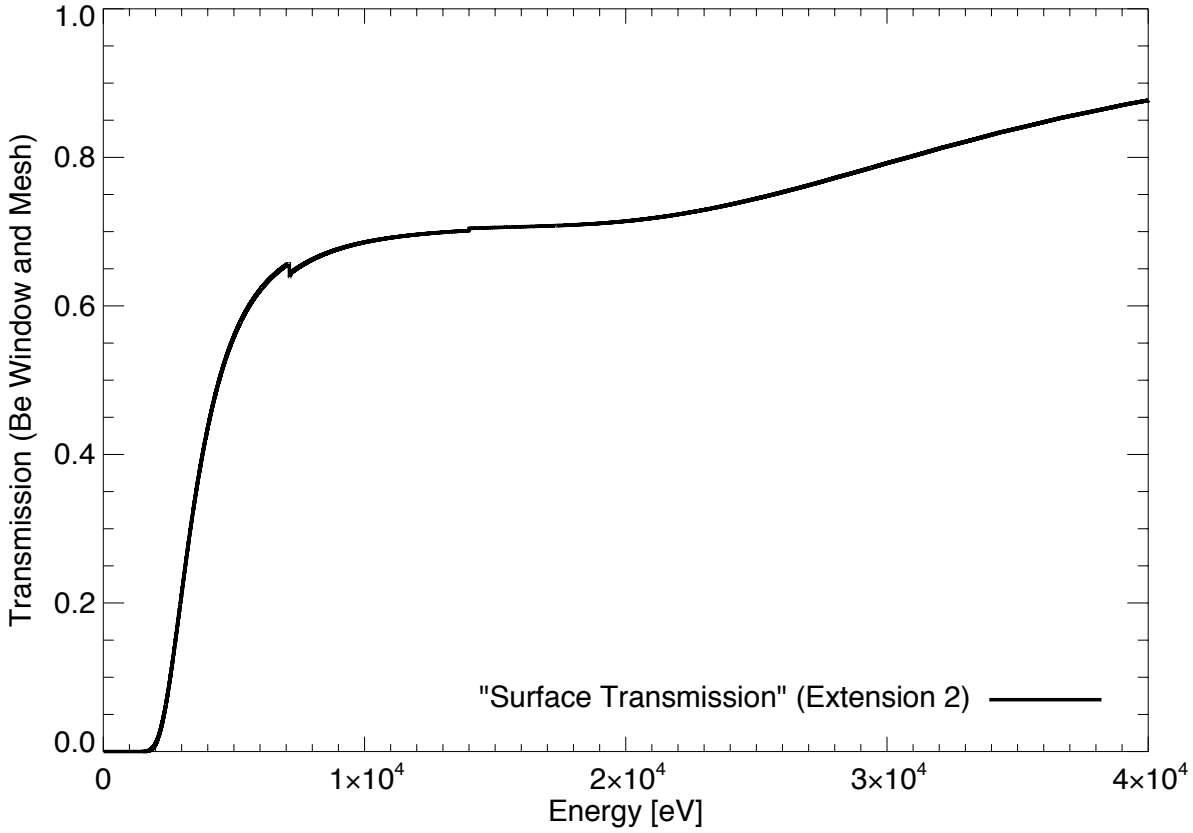


**Figure 9** Transmission of the GV beryllium window and stainless steel protective mesh (71% open area). These data are supplied on an 0.25 eV grid in Extension 2 of the CALDB file.

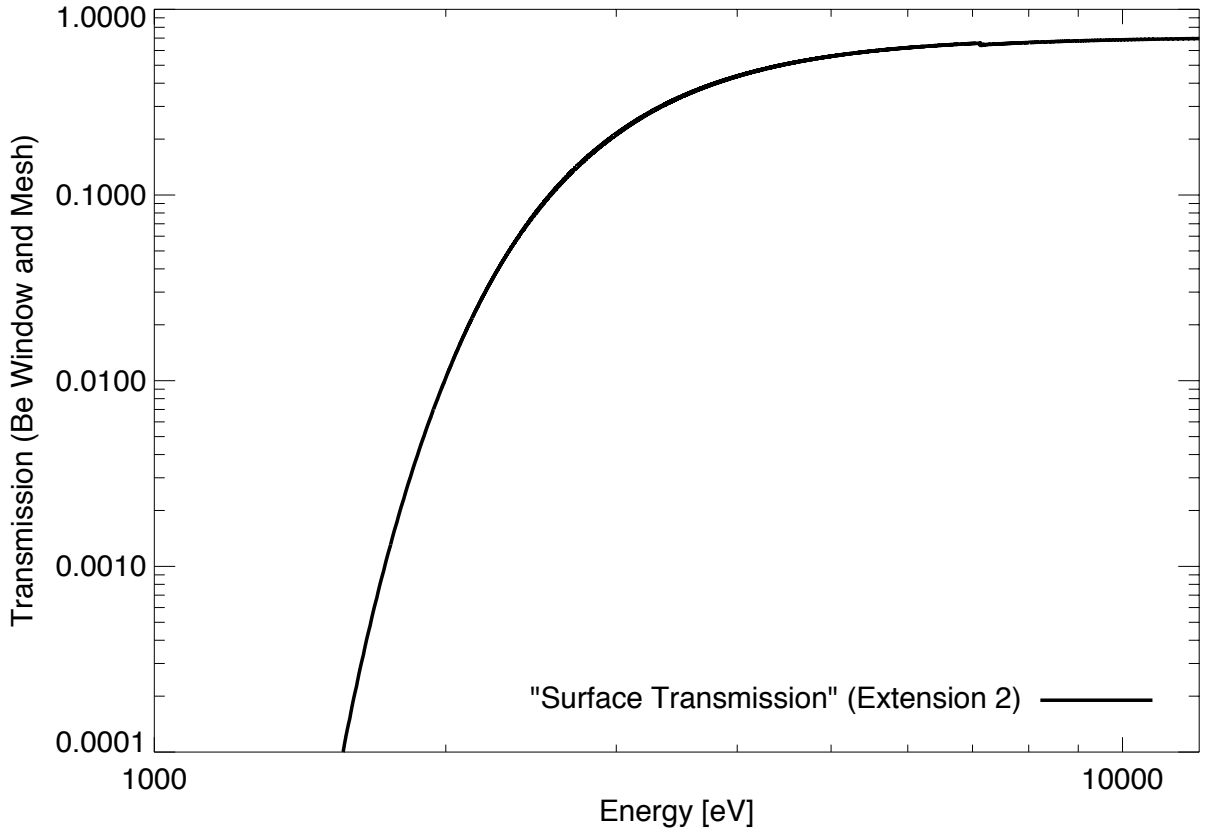


**Figure 10** Log-log plot of the **t**ransmission of the GV beryllium window and stainless steel protective mesh (71% open area) from 1–12 keV.

## 5 References

[1] B.L. Henke, E.M. Gullikson, and J.C. Davis. *X-ray interactions: photoabsorption, scattering, transmission, and reflection at E=50-30000 eV, Z=1-92*, Atomic Data and Nuclear Data Tables Vol. **54** (no.2), 181-342 (July 1993). http://henke.lbl.gov/optical_constants/asf.html

[2] SRON-ASTH-RP-2013-008, Characterizing the ASTRO-H Filters at Bessy

[3] http://www.nist.gov/pml/data/ffast/index.cfm

[4] C. T. Chantler. "Theoretical Form Factor, Attenuation and Scattering Tabulation for *Z*=1-92 from E=1-10 eV to E=0.4-1.0 MeV," *J. Phys. Chem. Ref. Data,* **24**, 71-643 (1995).

[5] C. T. Chantler. "Detailed Tabulation of Atomic Form Factors, Photoelectric Absorption and Scattering Cross Section, and Mass Attenuation Coefficients in the Vicinity of Absorption Edges in the Soft X-Ray (Z=30-36, Z=60-89, E=0.1 keV-10 keV), Addressing Convergence Issues of Earlier Work," *J. Phys. Chem. Ref. Data,* **29**(4), 597-1048 (2000).

[6] M.E. Eckart, et al. “Ground calibration of the Astro-H (Hitomi) soft x-ray spectrometer,” *Proc. SPIE,* **9905,** 99053W (2016). doi: 10.1117/12.2233053

[7] M.A. Leutenegger, et al. “In-flight verification of the calibration and performance of the ASTRO-H (Hitomi) Soft X-ray Spectrometer,” *Proc. SPIE,* **9905,** 99053U (2016). doi: 10.1117/12.2234230

[8] A. Hoshino, S. Kitamoto, R. Fujimoto, T. Ina, T. Uruga. “ASTRO-H/SXS spare Be Window evaluation result,” jaxa_sxs_memo_2016-013_v3.6.6 (2016-11-04).

[9] S. Stepanov, Online Bragg planes calculator, accessed 2016-10. http://x-server.gmca.aps.anl.gov/x0h_search.html